Title: A Comparative study on CdS: PEO and CdS: PMMA nanocomposite solid films

Author: S. Padmaja S. Jayakumar R. Balaji K. Vaideki

PII: S0025-5408(16)30131-3
DOI: http://dx.doi.org/doi:10.1016/j.materresbull.2016.03.026
Reference: MRB 8719

To appear in: *MRB*

Received date: 26-7-2015
Revised date: 18-3-2016
Accepted date: 21-3-2016

Please cite this article as: S.Padmaja, S.Jayakumar, R.Balaji, K.Vaideki, A Comparative study on CdS: PEO and CdS: PMMA nanocomposite solid films, Materials Research Bulletin http://dx.doi.org/10.1016/j.materresbull.2016.03.026

A Comparative study on CdS: PEO and CdS: PMMA nanocomposite solid films

S. Padmaja[1], *S. Jayakumar , R.Balaji [1], K.Vaideki [1]

[1]Thin film centre, PSG College of Technology, Coimbatore, India

* Department of Physics, PSG Institute of Technology and Applied Research, Coimbatore, India

Corresponding author:

Dr.S.Jayakumar
Department of Physics
PSG Institute of Technology and Applied Research
Neelambur
Coimbatore, India
Email: s_jayakumar_99@yahoo.com
Mobile: 09443157382

Graphical Abstract

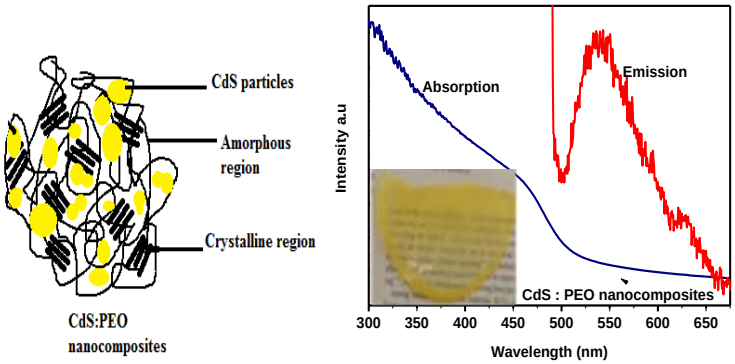

Absoprtion and Emission of translucent solid film

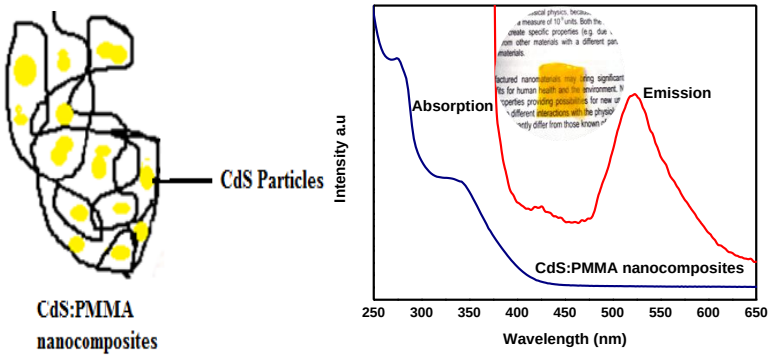

Absorption and Emission of transparent solid film

Abstract

Cadmium Suphide (CdS) nanoparticles were reinforced in Poly (ethylene Oxide) (PEO) and Poly (methyl methacrylate) (PMMA) matrices by insitu technique. The presence of CdS in PEO and PMMA matrix was confirmed using X-ray photoelectron spectroscopy (XPS). Fourier Transform Infrared spectroscopy (FTIR) analysis disclosed the co-ordination of CdS in the matrices. Thermal analysis of the nanocomposites was carried out using Differential Scanning calorimetric studies (DSC). The optical studies using UV-Visible spectroscopy were carried out to find the band gap of the materials and the absorption onset. The CdS particle size in the matrices was found by Effective Mass Approximation (EMA) model using the band gap values and was confirmed by TEM studies. The surface trapped emissions of the nanocomposites were observed from the photoluminescence (PL) spectra. The distribution of CdS particles in the polymer matrices were presented by Atomic force microscopic studies (AFM).

Keywords: Composites, Semiconductors, Optical materials, luminescence, Differential Scanning Calorimetry

1. Introduction

Polymer nanocomposites are new class of composites with nanoparticles as reinforcement. Different polymers are used with different filler particles to achieve various properties [1,2]. Polymers containing inorganic reinforcement do not scatter light and are interesting for optical applications [3,4]. Recent advances in controlling the fabrication and dispersion of semiconductor nanoparticles in the polymers have suggested possible uses in optical applications. From an application perspective, the dispersion as well as controlled segregation of nanoparticles within the solid matrix plays a vital role. The polymer materials used as matrix provide thermal and mechanical stability [5] making the nanocomposites an important candidate for widespread applications.

Recently, the semiconducting II-VI compounds such as CdS, CdSe, PbS and ZnS are receiving considerable attention. Especially Cadmium sulphide (CdS), a direct band gap semiconductor (E_g=2.4eV) can be used with polymer matrix for many optical applications which includes photo resistors, window layers in thin film solar cells, light detectors, LEDs and photoconductors [6,7]. Several researchers have reported the reinforcement of CdS particles in different polymer matrices to study its properties. P.K.Khanna and his group reported the light emission in blue-green and yellow-orange of visible spectrum using CdS/PMMA nanocomposites [8]. CdS colloid embedded in PEO matrix and its controlled blue light emission was reported by Chien-Ming Wei [9]. The nanocomposites were synthesized using solution based methods, colloidal route etc. But the reports on techniques to prepare transparent solid state materials preferable for device applications such as optical limiters, polymer/semiconductor solar cells and lenses are rare [10,11].

In the present study, we report the insitu preparation of CdS in PEO as well as in PMMA matrix. $Cd(NO_3)_2$ was used as a precursor to form solid films of $Cd(NO_3)_2$:PEO and $Cd(NO_3)_2$:PMMA. The films formed were then exposed to H_2S gas to convert it into CdS: Polymer nanocomposite. The solid films of minimum thickness with polymer itself as a capping agent were prepared. The structural, optical and thermal properties of the films were investigated and compared by different characterization techniques.

2. Materials and methods

2.11 Synthesis of CdS in PEO matrix and PMMA matrix

Poly(ethylene oxide) (M_W = $4x10^5$ g/mol), Poly(methyl methacrylate) (M_W = $3.5x10^5$ g/mol) and cadmium nitrate ($Cd(NO_3)_2.4H_2O$) were supplied by Aldrich for the preparation of nanocomposites. Initially, PEO was dissolved in 50 ml of acetonitrile and stirred continuously using a magnetic stirrer. After vigorous stirring, $Cd(NO_3)_2.4H_2O$ was added to the PEO solution and stirred further for the homogeneous distribution of $Cd(NO_3)_2$ in PEO matrix. The concentration of $Cd(NO_3)_2$: PEO was taken in 1:100 molar ratio. The solution was then transferred to petri dishes and dried to form thin solid films by completely evaporating the solvent. The dried films were then exposed to H_2S gas from a Kipp's apparatus for half an hour. The films slowly changed from white colour to yellow which was the indication of the formation of CdS. The same procedure was adopted for synthesizing CdS in PMMA (1:100 molar ratio) matrix. The only difference is, PMMA was dissolved in 50ml of tetra hydro furan instead of acetonitrile. Finally the transparent yellow films of CdS: PMMA was obtained.

The prepared films were subsequently characterized. The thickness of the films was found by interferometric method. The compositional analysis was done by X-ray photo electron spectroscopy (XPS VG ESCA MK200X). Interaction of CdS with the functional group of polymer was discussed using Fourier Transform Infrared spectroscopy-Attenuated Total Reflectance (FTIR-ATR) (Spectrum 100, Perkin-Elemer, and Spectro- meter). The thermal properties of the polymer nanocomposite solid films were analysed by Differential Scanning Calorimetry (TA instruments DSC Q20). The films were characterized using UV-Visible spectroscopy (UV-Vis Cary5E) to find the band gap of the material and the particles size were estimated from the Effective Mass Approximation (EMA) model. To confirm the quantum confinement, the emission from Photoluminescence spectroscopy (Jobin Yvon FL3-11) was used. The particles size was estimated from the Transmission electron microscope (JEOL 2100) (operated at 80KV) and for the particle distribution of the composites, Atomic Force Microscope (NT-MDT model) was used.

3. Results and discussions:

The obtained CdS: PEO solid films and CdS: PMMA solid films were both yellow in colour but the later was more transparent (Fig. 1a and 1b). The thickness of the solid films using interferometric method was found to be ~10 μm and ~5 μm, respectively. It is well known that PEO is a partially crystalline polymer and the crystallinity of the polymer makes the nanocomposite to appear translucent. By further reducing the thickness of the solid films of CdS:PEO composites the transparency can be improved.

XPS measurements were carried out to confirm the presence of CdS in the polymer matrix. Fig.2a. shows the photoelectron spectrum of Cd3d for CdS:PEO and CdS:PMMA

nanocomposites. The peaks present at 406.04eV for CdS:PEO and 405.59 eV for CdS:PMMA were attributed to $Cd3d_{5/2}$ peaks. The peaks present at 412.84 eV for CdS:PEO and 412.36 eV for CdS:PMMA were attributed to $Cd3d_{3/2}$ peaks [12] and small binding energy shift is observed between the composites. The shift of Cd3d peak in CdS:PMMA composite may be attributed to the reduction in size of the particles in the matrix or due to the moiety. However the shift is negligible. Fig.2b shows the S_2p peaks of the composites at 162.62 eV for CdS:PEO and 163.38 eV for CdS:PMMA which were in good agreement with the binding energy of sulphur [13]. The peaks were deconvoluted and the ratio of elemental Cd:S was found to be 0.83:1.14 and 1.05:0.96 in PEO and PMMA nanocomposite. In both the composites the elemental ratio of Cd:S was close to 1:1 [14].

The interaction of Cd^{2+} with PEO matrix and with PMMA matrix before and after exposure of H_2S gas was studied by FTIR spectra (Fig.3a.). In pure PEO matrix, the strongest peak present at 1097 cm^{-1} was attributed to C-O-C stretching mode. The vibrational mode at 960 cm^{-1} was attributed to CH_2 rock and CH_2 twist while the CH_2 rocking and C-O stretching vibrational mode was observed at 842 cm^{-1}. The position of the peaks were unaffected by the addition of Cd^{2+} in the matrix. Fig.3b shows the relative intensity ratio of peaks with C-O-C stretching peak. Comparing with pure PEO peaks, when Cd $(NO_3)_2$ was added, there was an increase in the relative intensity ratio of all the peaks [15] and this confirms the interaction of Cd^{2+} with PEO. When the film was exposed to H_2S gas, all the Cd^{2+} ions were converted to CdS. PEO was not able to complex it as much as ionic Cadmium and so the peaks of CdS:PEO came back nearly to the same position of the pure PEO . This is the indication of neutralized CdS particles which were frozen up at the particular position in the polymer chain.

In CdS: PMMA nanocomposite (Fig.3c.) the strongest peak corresponding to carbonyl functionality C=O was observed at 1724 cm^{-1}. The peak at 1145 cm^{-1} corresponds to C-O-C stretching vibrations and 1435 cm^{-1} corresponds to bending vibration of PMMA. Fig.3d shows the relative intensity ratio of other peaks with C-O-C stretching peak with unaffected peak positions. Compared to pure PMMA, when Cd^{2+} was added, the increase in the relative intensity ratio of the strongest peaks informed the coordination of Cd^{2+} with PMMA [16]. When the sample was exposed to H_2S gas, there is a slight decrease in the relative intensity ratio of the peaks which is in contrast to the PEO matrix. In order to understand the complete mechanism of crystalline and amorphous matrix, the samples were subjected to DSC studies.

DSC analysis was carried out from 30^0C to 80^0C for pure PEO, $Cd(NO_3)_2$:PEO and for CdS:PEO (Fig.4a). All the PEO samples exhibit similar pattern except the peak position. The peak is attributed to the melting point of PEO. For pure PEO, the endothermic peak present at 65^0C was accompanied with the change in enthalpy of 201J/g (percentage of crystallinity was 94%). In the presence of $Cd(NO_3)_2$, the melting point was reduced to 61^0C with the change in enthalpy of 20.20J/g (percentage of crystallinity was 10%). About 90% of the crystalline polymer was transformed to amorphous nature by the addition of Cd^{2+}. The degree of crystallinity was determined from the relation $\mathbf{X_c\ (\%) = (\Delta H_m/\Delta H_{m0})\ x\ 100,}$ where ΔH_m is the melting enthalpy estimated experimentally and ΔH_{m0} is the melting enthalpy for 100% crystalline PEO (213.7 J/g) [17]. The calculated values were tabulated in table 1.

It is evident that the Cd^{2+} ions coordinated to the back bone of the polymer chain and the crystallinity of the polymer decreases and so the melting point shifts towards lower temperature due to colligative nature. Once all the Cd^{2+} ions has been converted to CdS the bounded Cd^{2+}

ions loses its influence in the polymer chain. This results in charge neutralized CdS which does not have any interaction with the polymer chain and so the melting peak came back nearly to the same position of pure PEO peak at 65^0C with the change in enthalpy of 27.41J/g and with the percentage of the crystallitnity around 13%. There was a negligible rise in crystallinity for CdS reinforced PEO (CdS: PEO) composites. The discussions were in agreement with the FTIR results where the peaks of CdS:PEO came back to the same position of pure PEO.

Fig.4b show the glass transition temperature of a highly amorphous PMMA polymer, $Cd(NO_3)_2$: PMMA and CdS:PMMA their corresponding glass transition temperatures were tabulated in table 2. The glass transition temperature of pure PMMA was around 112 ^{o}C (taken in the mid of the slope).

In the presence of Cd^{2+}, the free volume of the amorphous PMMA decreases and the segmental motion of the polymer chains were restricted by the Cd^{2+}. So the composite turned hard and the glass transition temperature increases to 139 ^{o}C. When the material was exposed to H_2S gas, the glass transition temperature was observed at 133 ^{o}C which is very close to the glass transition temperature of $Cd(NO_3)_2$: PMMA[18] . This indicates that once the amorphous materials are synthesized, the hardness of the material remains unchanged. Hence, the FTIR results for PMMA-CdS, shows the slight decrease in intensity ratio.

Fig.5a and 5b shows the UV-Visible absorption and emission spectrum of CdS:PEO and CdS:PMMA composites. It was found that the absorption spectrum of CdS:PEO composites was accompanied by the absorption band edge at 505 nm with the excitonic shoulder at 470 nm corresponding to the band gap of 2.47 eV. The band gap values of CdS:PEO composites were identified from $(\alpha h\nu)^2$ vs $h\nu$ plot (Fig.5c). The blue shift of the absorption spectrum from the

bulk band edge of CdS (512 nm with band gap 2.4 eV) suggests the quantum confinement. The CdS crystallite size estimated from the effective mass approximation model (EMA) [19] was 5 nm. The corresponding emission spectrum was broad and centered at 541 nm. The broadened emission spectrum indicated the surface defects and multimodal distribution of crystallites in the matrix [20].

The absorption spectra of CdS:PMMA composites exhibits two shoulders at 274 nm and at 341nm corresponding to the band edge of 420 nm respectively. The band gap of the CdS:PMMA composites from $(\alpha h\nu)^2$ vs $h\nu$ plot (Fig.5c) was 3.09 eV . The two absorption shoulders observed in the spectra may be due to the different size of CdS crystallites present in the matrix [21]. The particles size calculated from the EMA model was 2 nm and in the strong confinement regime. The emission spectra showed a small near band edge emission hump at 425 nm and broad spectra centered at 522 nm. Though the band edge difference between CdS:PEO and CdS:PMMA nanocomposites are around 85 nm(505 nm to 420 nm) the emission spectra shows only 20 nm difference. This confirms the trapped emission for CdS:PMMA nanocomposites.

The samples for TEM were prepared by dipping the copper grids directly in the solution containing $Cd(NO_3)_2$:PEO and $Cd(NO_3)_2$:PMMA.The solution was dried for few minutes and then exposed to H_2S gas. The grids were then placed in the TEM chamber for recording the transmission image.

In PEO matrix (Fig.6a), the CdS particles were evenly distributed and are in the spherical shape. The few agglomerations may be due to the fast mobility and rapid growth of particles in the polymer matrix [22]. CdS particle size can be estimated to be 25 to 30 nm, which represented

an agglomeration of about 5-6 crystallites which were in good agreement with the particle size calculated from the EMA model. The Fig.6b. shows the CdS particles in PMMA matrix. Because of Ostwald ripening smaller particles combined together to form aggregates and the crystallite sizes were in the range 30-40 nm with aggregation of 15 to 20 crystallites. Smaller the particle size, larger the surface area which leads to aggregation of particles [23].

Fig.7 shows the AFM images of CdS: PEO nanocomposites. The phase image depicts the distribution of CdS particles in PEO matrix. The enlarged view of CdS particles in the particular box area shows the minimum size distribution of particles. The height profile represents the minimum particle size of 15 nm and maximum of 50 nm. The particles size may also be contributed by the organic part of the sample or the aggregation of the smaller particles.The average roughness of the CdS:PEO nanocomposite solid film was 56 nm [24].

The AFM images of CdS:PMMA nanocomposite solid films were represented in fig.8. The images clearly displays the CdS particles distributed in PMMA matrix. The height profile represented the average distribution of particles and it is around 10 to 25 nm and the maximum of 35 nm which agrees with the particle size calculated from TEM . The average roughness of the CdS:PMMA nanocomposite solid films was around 29 nm. The surface roughness of CdS:PMMA is less compared to that of CdS:PEO nanocomposite solid films. Both nanocomposites reveal uniform distribution of particles in the matrix. However CdS:PMMA consists of narrow size distribution compared to that of CdS:PEO nanocomposite [25].

4. Conclusion

We have presented the synthesis and characterization of CdS:PEO and CdS:PMMA naocomposite solid films and also their properties are analysed and compared. The

nanocomposite solid film prepared out of CdS:PMMA was transparent whereas the CdS:PEO nanocomposite solid film was translucent and the quality of the film should be improved to obtain good transparency. The thermal analysis reveals that the melting temperature of the CdS:PEO nanocomposites is less compared to pure PEO and there is no significant change in the percentage of crystallinity before and after H_2S treatment. In CdS:PMMA nanocomposites before and after H_2S treatment, the glass transition temperature of nanocomposites increases which in turn increases the hardness of the composites. Thermal stability of CdS:PMMA nanocomposites was elucidated from the above results. The band gap of CdS:PEO nanocomposite is 2.47eV and for CdS:PMMA nanocomposite it is 3.09eV. The wide tuning of bandgap in CdS:PMMA nanocomposite and the particle size discloses the good qunatum confinement. AFM results confirmed the uniform and narrow distribution of particles in CdS:PMMA nanocomposite compared to CdS:PEO nanocomposite. On comparison of these two CdS incorporated polymers, CdS:PMMA nanocomposite solid films with high transparency can be preferred for optoelectronic device applications .

Acknowledgement

The authors would like to thank the Principal and Management, PSG College of Technology for the support extended towards this research work.

References:

[1] J. Kuljanin-Jakovijevic, Z.Stojanovic, J.M.Nedeljkovic, 'Influence of CdS – filler on the thermal properties of poly(methylmethacrylate), J.Mater.Sci. 2006,**41,** 5014-5016

[2] T.Radhakrishnan,M.K.Georges,P.Sreekumari,A.S.Luyt,V.Djokovic, 'Composites comprising CdS nanoparticles and poly(ethylene oxide): optical properties and influence of the nanofiller content on the thermal behaviour of the host matrix', Colloid Polym Sci., 2008, **286,**683-689

[3] A.A.Biryukov,T.I.Izaak,E.Yu. Gotovtseva,I.N. Lapin,A.I. Potekaev,V.A.Svetlichnyi,'Optical properties of CdS/MMA dispersions and CdS/PMMA nanocomposites prepared by one-step size controlled synthesis', Russian Physics Journal., 2011, **53**,849-856

[4] I.Umezu,R.Koizumi,K.Mandai,T.Aoki-atsumoto,K.Mizuno,M.Inada,A.sugimura,Y.Sunaga,T.Ishii,Y.Nagasaki, 'Optical properties of CdS nanocrystal covered by polymer chains on the surface'**,** Microlectronic Engineering., 2003,**66**, 53-58

[5] F.Antolini,E.Burresi,V.M orandi,L.Ortolani,G.Accorsi,M.Blosi, 'Time and Temperature Dependence of CdS Nanoparticles Grown in a Polystyrene Matrix', Journal of Nanomaterials., 2012 **, 2012**, 1-11

[6] Muhammad Arshad Kamran, Ruibin Liu, Li-Jie Shi, Arfan Bukhtiar, Jing Li, and Bingsuo Zou, 'Synthesis of Novel Sea-Urchin-Like CdS and their optical properties', J.Nanoscience and Nanotechnology., 2015,**15** 4435-4441

[7] C.S. Pathak, M.K.Mandal , V.Agarwala, 'Optical properties of undoped and cobalt doped ZnS nanophosphor', Materials Science in semiconductor processing., 2012, **16** ,467-471

[8] P.K.Khanna, Narendra Singh, **'**Light emitting CdS quantum dots in PMMA: Synthesis and optical studies', Journal of luminescence., 2007,**127 ,** 474-482

[9] Chien-Ming Wei,Sheng-Shu Hou, 'Preparation and optical properties of blue-emitting colloidal CdS nanocrystallines by the solvothermal process using poly (ethylene oxide) as the stabilizer',Colloid Polym Sci., 2007, **285** ,1343-1349

[10] Jie Jiao, Zheng-Ji Zhou, Wen-Hui Zhou, Si-XinWun, ' CdS and PbS quantum dots co-sensitized TiO2 nanorod

arrays with improved performance for solar cells application', Materials Science in semiconductor processing., 2013,**16,** 435-440

[11] Guangming Liu, T.Schulmeyer, J.Brotz, A.Klein, W.Jaegermann, 'High Efficiency and cost effective Cu2S/CdS thin-film solar cell' Thin Solid films., 2003,**477**, 431- 432

[12] Jun Yao, Mei Yang, Yu Liu, and Yixiang Duan, 'Flourescent CdS quantum dots: Synthesis, characterization,mechanism and interaction with gold nanoparticles, J.Nanoscience and Nanotechnology., 2014,**15**, 3720-3727

[13] Marisol Tejos, Barbara G.Rolon, Rodrigo del Rio, Gerardo cabello, 'CdS amorphous thin films photochemical synthesis and optical characterization', Materials Science in Semiconducting Processing, 2008,**11**, 94-99

[14] G.Z.Wang, Y.W. Wang, W.Chen, C.H.Liang, G.H.Li, L.D.Zhang, 'A Facile synthesis route to CdS nanoparticles at room temperature', Materials Letters, 2001, **48**, 269-272

[15] Xuefeng Ding, Zichen Wang, Dongxue Han, Yuanjian Zhang, Yanfei Shen, Zhijuan, Wang,Li Niu, 'An effective approach to synthesis of poly(methyl methacrylate)/silica nanocomposites', Nanotechnology., 2006, **17**, 4796-4801

[16] Hongmei Wang, Pengfei Fang, Zhe Chen, Shaojie Wang, 'Synthesis and Characterization of CdS/PVA nanocomposite films, Applied Surface Science.,2007, **253,** 8495-8499

[17] Jing Zhao,Xingming Shuai,Li wang, Xinqiang Tang, Xinhua Xu, Jing Sheng,Dinghai Huang, 'The thermodynamic behavior and morphology of PP/POE blends prepared by melt- and solution- mixing methods', J.Mater Sci., 2009,**44** , 2171-2175

[18] Liyun Ding, Tao Li, Yunmin Zhong, Chao Fan, Jun Huang, Materials Science and Engineering C, **'**Synthesis and characterization of a novel nitric oxide fluorescent probe cds-pmma nanocomposite via in-situ bulk polymerization', 2014,**35**, 29-35

[19] L.E. Brus,' Electronic wave functions in semiconductor clusters: experiment and theory'**,** J. Phys. Chem., 1986,**90,**(12) 2555-2560

[20] Hooi Lind Lee, Issam Ahmed Mohammed, Mohammed Belmahi, Mohammed Bedreddline Assouar, Herve Rinnert, Marc Alnot, Materials, 'Thermal and optical properties CdS nanoparticles in thermotropic liquid crystal monomers'., 2010 **3**, 2069-2086

[21] Jie Zhao, Fanghong Yang, and Ping Yang, 'Growth of CdS nanorods and deposition of silver nanoparticles', J.Nanosceince and Nanotechnology, 2015,**15**, 3928-3923

[22] O. P. Sinha, Ritu srivatsava, T. Shripathi, , 'Synthesis and characterization of CdS crystal dispersed in polymer Matrix, Nano:Brief Reports and Reviews., 2010, **5**, 97–102

[23] S.Meenakshi Sundar, C.K. Mahadevan, P. Ramanathan, **'**On the Preparation of ZnO–CdO Nanocomposites Materials and Manufacturing Processes', 2007, **22**, 400-403

[24] S. Lewis, V. Haynes, R. Wheeler-Jones, J. Sly, R.M. Perks, L. Piccirillo, 'Surface characterization of poly (methylmethacrylate) based nanocomposite thin films containing Al_2O_3 and TiO_2 nanoparticles, Thin Solid films, 2010,**518** , 2683-2687

[25] M.Thambidurai, N.Muragan, N.Muthukumarawamy, R.Vasantha, R.Balasundaraprabhu, S.Agilan, Preparation and characterization of nanocrystalline cds thin films',Chalcogenide Letters., 2009,**6 ,**171-179
Chalcogenide Letters, **6** (2009)171- 179

Figures

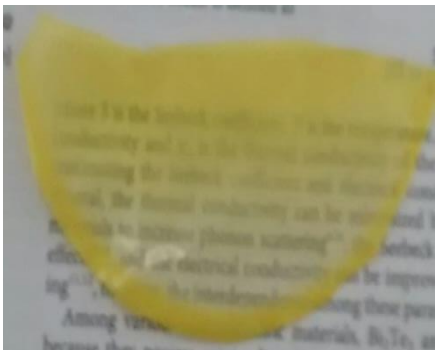

Fig.1a. CdS: PEO nanocomposite solid film (yellow and partially transparent film)

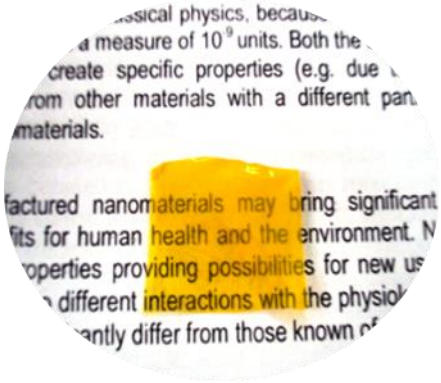

Fig.1b. CdS: PMMA nanocomposite solid film (yellow transparent film)

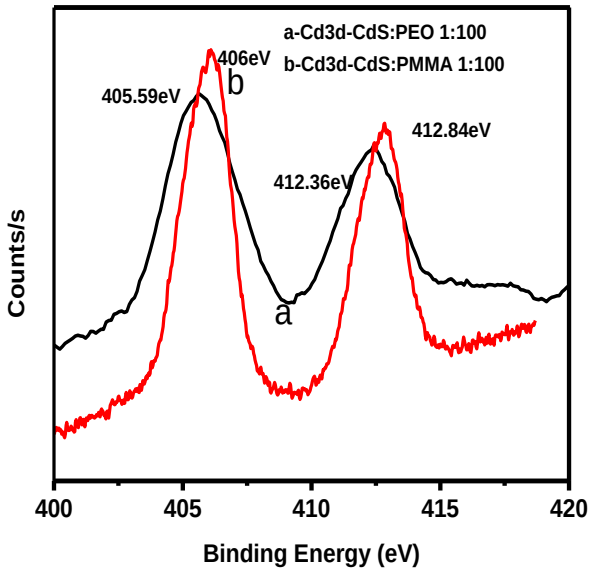

Fig.2a. XPS (Cd3d) spectra of CdS:PEO and CdS:PMMA nanocomposites

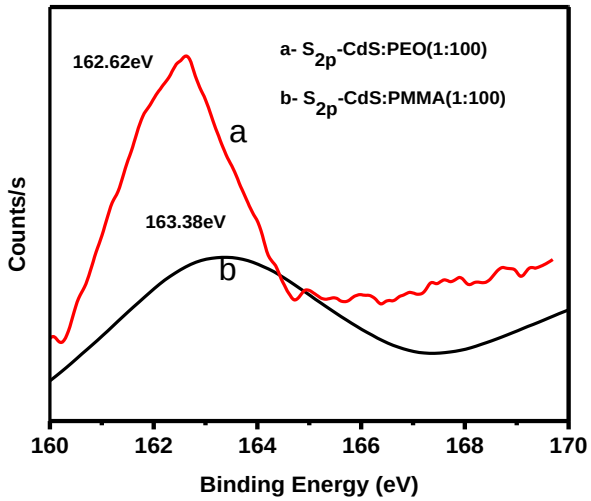

Fig.2b. XPS spectra of CdS:PEO and CdS:PMMA nanocomposites (S_2p core)

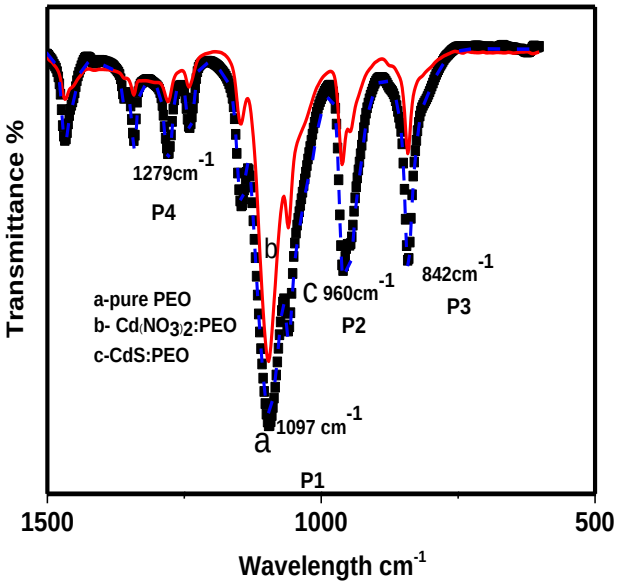

Fig.3a. FTIR-ATR spectra of CdS:PEO nanocomposites a)Pure PEO b) before H_2S treatment c)After H_2S treatment

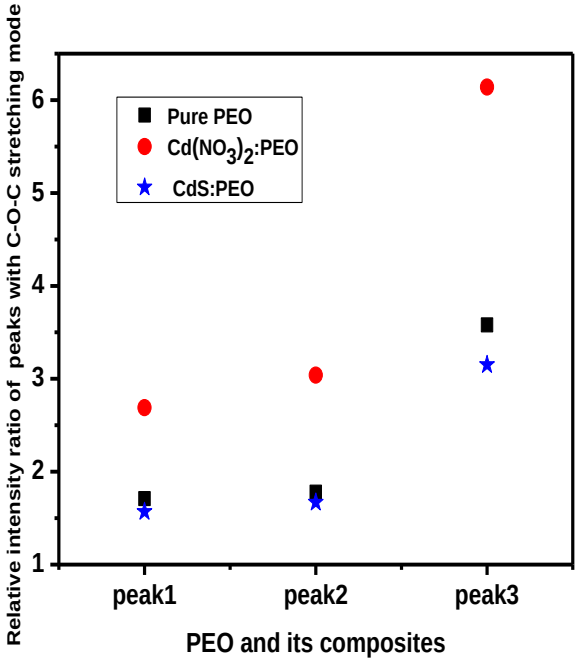

Fig.3b. Relative intensity ratio of peaks of CdS:PEO nanocomposites with C-O-C stretching peak

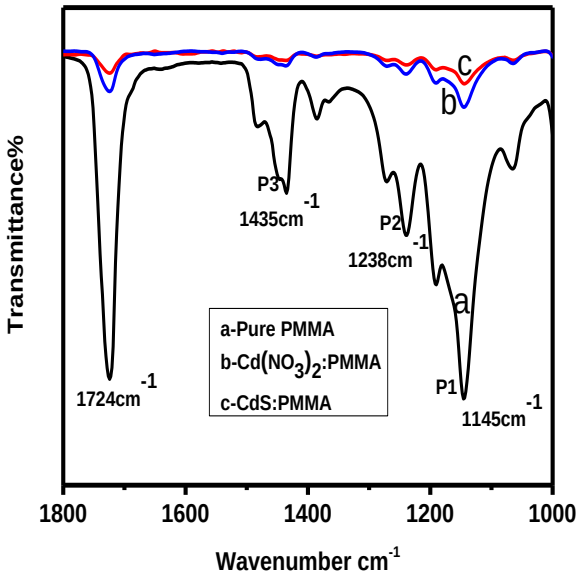

Fig.3c. FTIR-ATR spectra of CdS:PMMA nanocomposites a)Pure PMMA b)before H_2S treatment c) after H_2S treatment

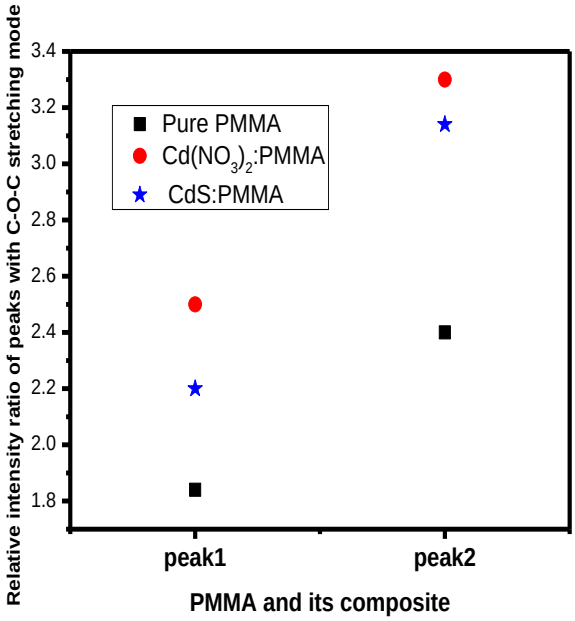

Fig.3d. Relative intensity ratio of peaks of CdS:PMMA nanocomposites with C-O-C stretching peak

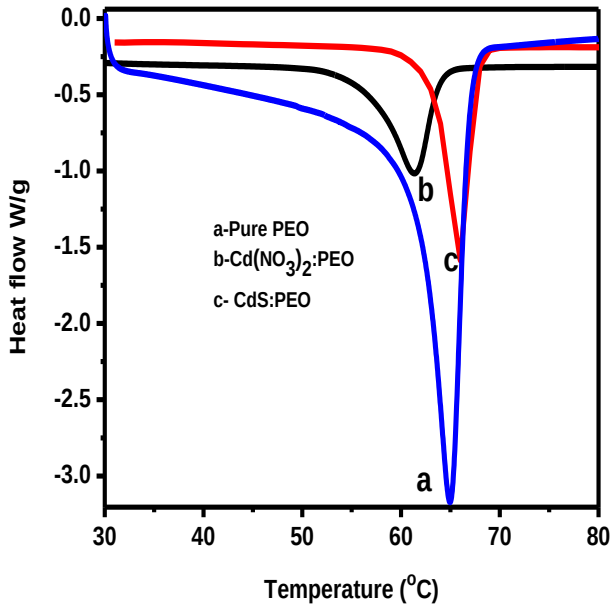

Fig.4a. DSC curves of PEO nanocomposites a) Pure PEO b) before H_2S treatment c) After H2S treatment

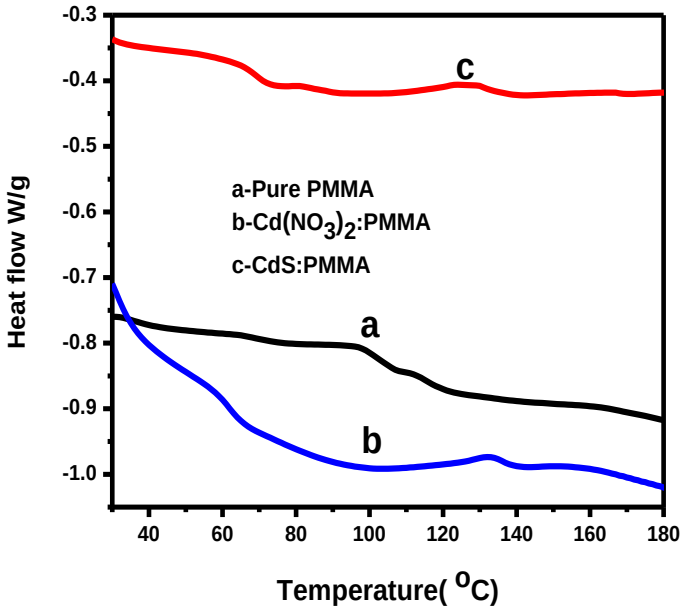

Fig.4b. DSC curves of PMMA nanocomposites a)Pure PMMA b) before H_2S treatment c) After H_2S treatment

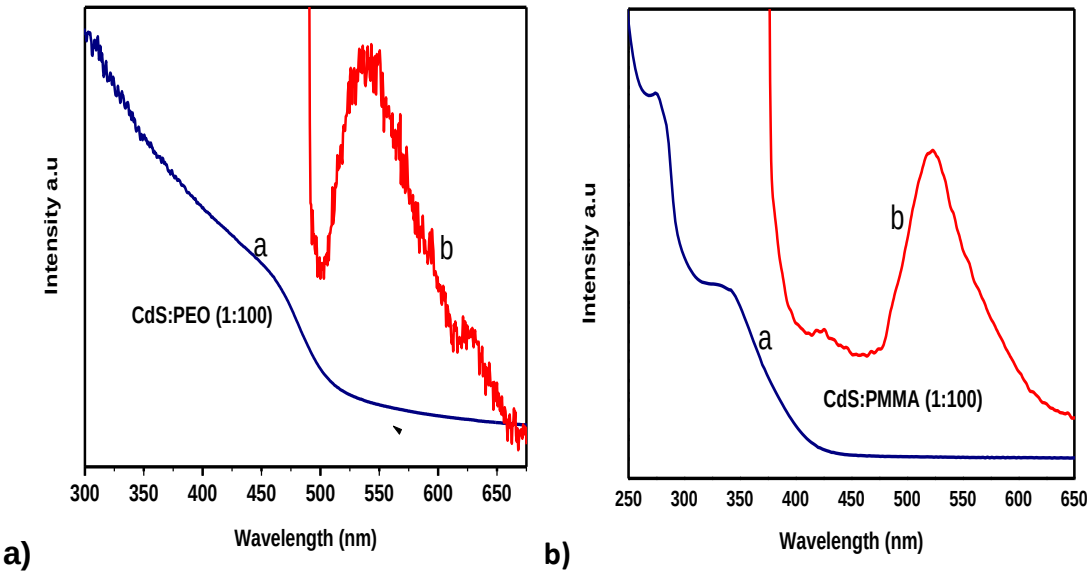

Fig.5. Absorption (a) and b) Emission spectra of CdS:PEO and CdS:PMMA nanocomposites

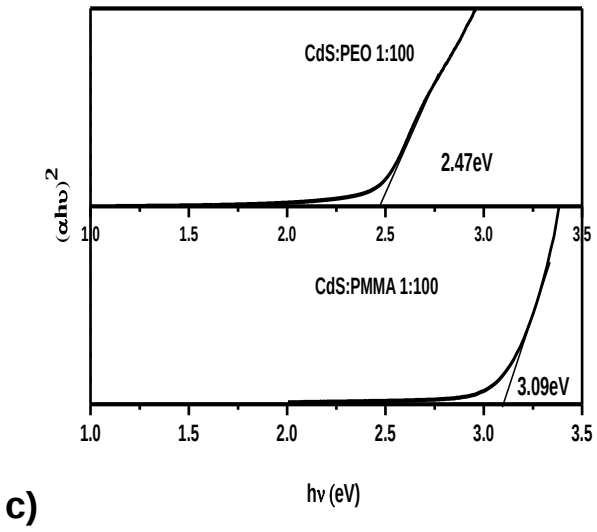

Fig.5c. $(\alpha h\nu)^2$ Vs $h\nu$ plot for CdS:PEO and CdS :PMMA nanocomposites

a) 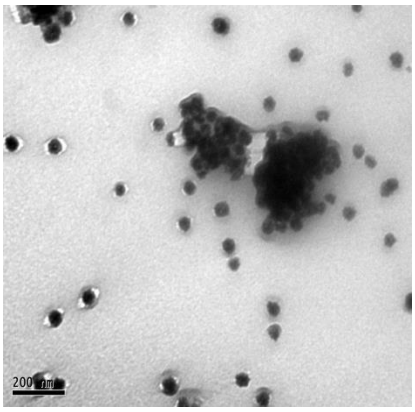

b) 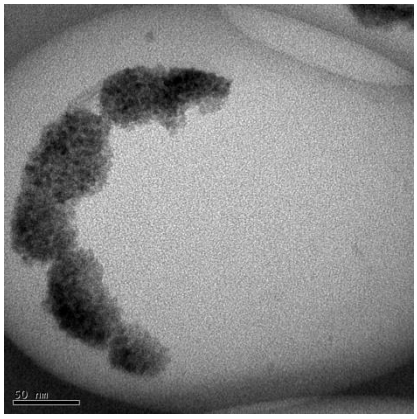

Fig.6.TEM image of a)CdS : PEO b)CdS : PMMA nanocomposites

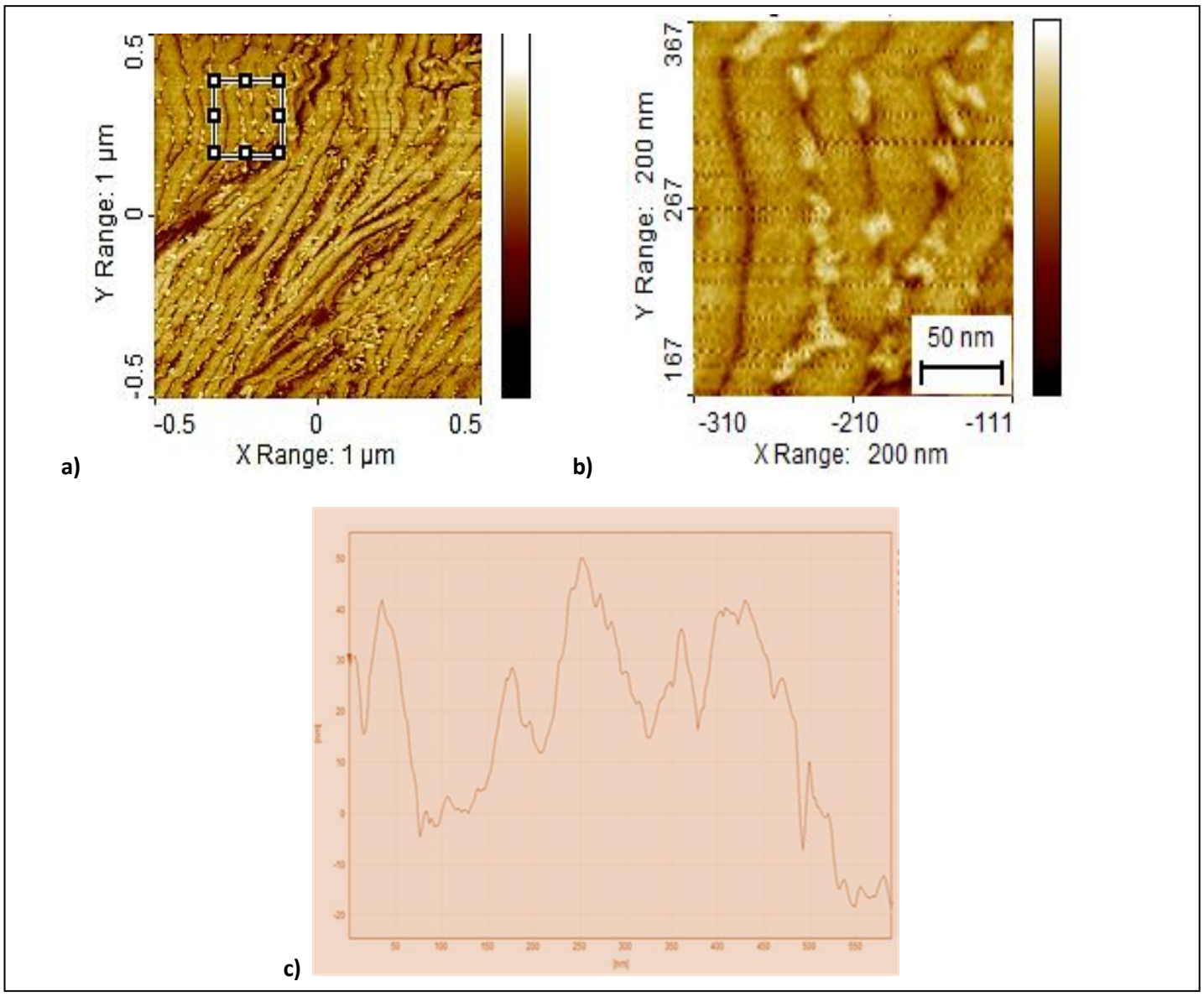

Fig.7. a) AFM phase image of CdS:PEO nanocomposite b) enlarged view of the CdS particles in the particular box area c) height prof the CdS particles in the matrix at two different places.

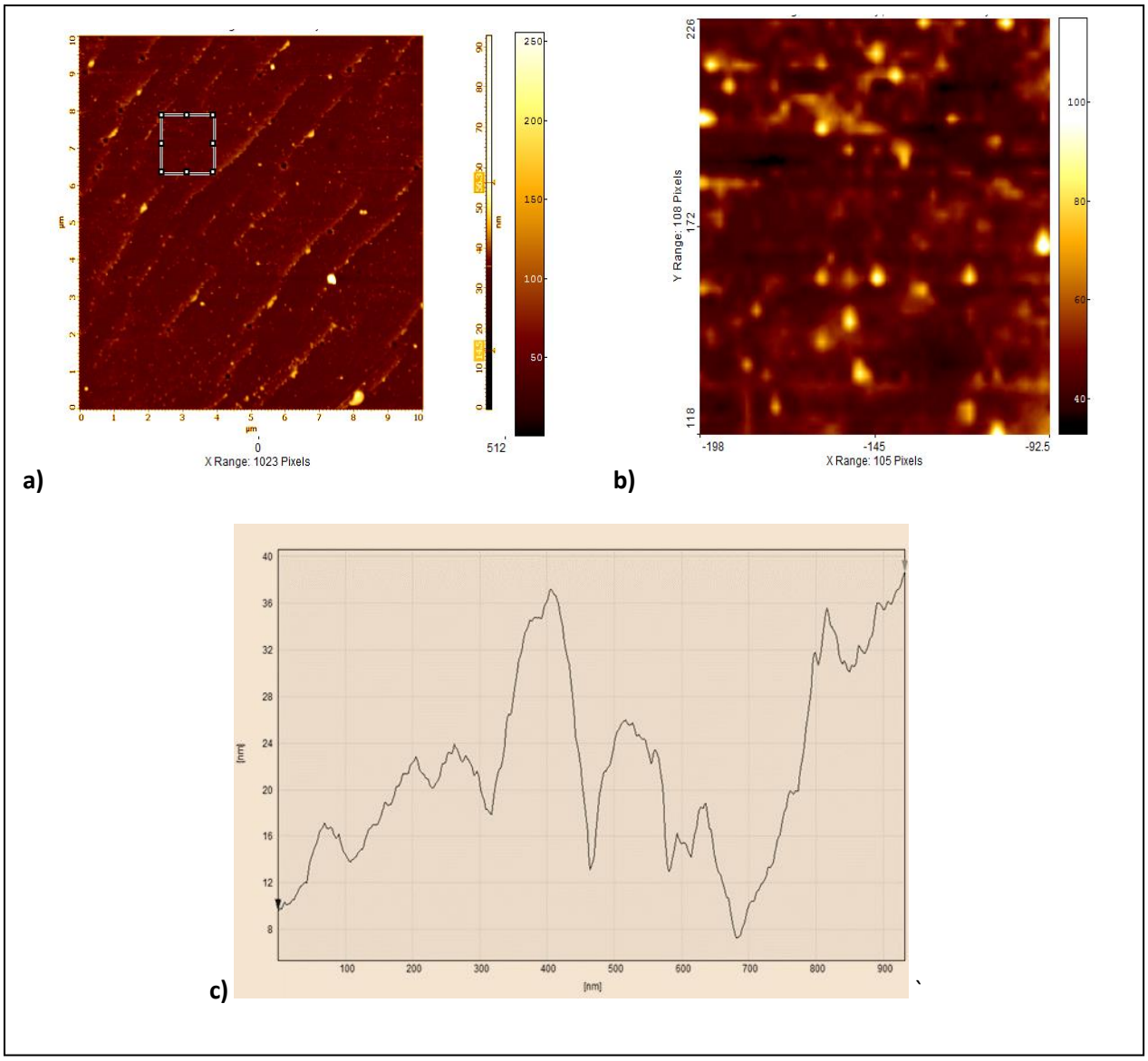

Fig.8. a)AFM phase image of CdS:PMMA nanocomposite b) enlarged view of the CdS particles in the particular box area c) height profile of the CdS particles in the matrix at two different places.

TABLES

Table 1: Melting point and % of crystallinity for CdS:PEO polymer composites

Polymer/Composite	**Melting point (T_m ^{0}C)**	**Enthalpy(J/g) (ΔH_m)**	**% of crystallinity (%)**
Pure PEO	65	201	94%
$Cd(NO_3)_2$: PEO	61	20.20	9.4%
CdS : PEO	65	27.41	12.8%

Table 2: Glass transition temperature for CdS:PMMA polymer composites

Polymer/Composite	**Glass transition temperature(T_g)** **(^oC)**
Pure PMMA	112
$Cd(NO_3)_2$: PMMA	139
CdS:PMMA	133